NBSIR 80-2177

Generation and Measurement of DC Electric Fields With Space Charge

Martin Misakian

Electrosystems Division
Center for Electronics
and Electrical Engineering
National Bureau of Standards
U.S. Department of Commerce
Washington, DC 20234

November 1980
Issued January 1981

Under Department of Energy Contract No. EA-77-01-6010
Task No. A018-EES

Prepared for:
Electric Energy Systems Division
Department of Energy

NBSIR 80-2177

GENERATION AND MEASUREMENT OF DC ELECTRIC FIELDS WITH SPACE CHARGE

Martin Misakian

Electrosystems Division
Center for Electronics
and Electrical Engineering
National Bureau of Standards
U.S. Department of Commerce
Washington, DC 20234

November 1980
Issued January 1981

Under Department of Energy Contract No. EA-77-01-6010
Task No. A018-EES

Prepared for:
Electric Energy Systems Division
Department of Energy

U.S. DEPARTMENT OF COMMERCE, Philip M. Klutznick, *Secretary*
Jordan J. Baruch, *Assistant Secretary for Productivity, Technology, and Innovation*
NATIONAL BUREAU OF STANDARDS, Ernest Ambler, *Director*

ABSTRACT

Characterization of the electrical environment in the vicinity of high voltage dc transmission lines requires measurement of a number of electrical parameters associated with the lines. These parameters include the electric field strength with significant space charge contributions. This report describes an experimental effort to generate known dc electric fields containing controlled amounts of space charge. An apparatus which has been built for this purpose is described and two types of field probes currently used for transmission line field measurements are examined with the apparatus. Limitations on the operation of one type of probe in the presence of very large current densities are identified and discussed.

TABLE OF CONTENTS

GENERATION AND MEASUREMENT OF DC ELECTRIC FIELDS WITH SPACE CHARGE

I. INTRODUCTION

With the gradual growth of dc transmission of electrical energy has also come an interest for a full characterization of the electrical environment in the vicinity of high voltage dc (HVDC) transmission lines. Because some corona is usually associated with normal operation of HVDC lines this environment is complicated by the presence of space charge. The electrical parameters of primary interest are currently thought to include[1] the electric field strength $\vec{E}$, with significant space charge contributions, the current density $\vec{J}$, and the space charge density ρ. At the present time probes used for the measurement of HVDC transmission line electric fields at ground level are calibrated with space-charge-free (ρ=o) fields produced between parallel plates. The probes are subsequently used to measure electric fields which may exceed 30 kV/m in the presence of space charge current densities[1,2] as large as 0.1 $\mu A/m^2$. It is noteworthy that future dc transmission systems, as well as biological exposure systems presently under consideration, may produce fields and current densities which are greater than the above values.

This paper describes an experimental effort to generate known dc electric fields with space charge. Experimental uncertainties are noted and are used to estimate the possible error in calculated values of electric field strength produced by a parallel plate apparatus. The apparatus has been used to examine the performance of two types of commonly used electric field probes, namely, an electric field mill[3] and two commercial vibrating-plate

probes[3]. While there have been earlier reports of laboratory apparatus which generate dc electric fields with space charge[2,4], this work focuses more on the problems associated with producing an electric field of known magnitude.

II. APPARATUS AND THEORY

In deciding on the design for an apparatus, several electrode geometries were examined. The electric field in each case satisfies Poisson's equation,

$$\nabla \cdot \vec{E} = \rho/\varepsilon_o \quad , \tag{1}$$

and the constitutive relation for the conduction current density

$$\vec{J} = \rho k \vec{E} \quad , \tag{2}$$

where ε_o is the permittivity of free space and k is the ion mobility. Because corona in air will generate several ion species[5,6], Eq. (2) must be modified to

$$\vec{J} = (\Sigma \rho_i k_i)\vec{E} \tag{3}$$

where ρ_i and k_i are the charge density and mobility of the i^{th} charge carrier species respectively. Expressing

$$\rho_i = \alpha_i \rho \tag{4}$$

where α_i is the fraction of the total charge density attributable to the i^{th} charge carrier, Eq. (3) can be written

$$\vec{J} = \rho(\Sigma\alpha_i k_i)E = \rho K\vec{E} \tag{5}$$

where K is the weighted average of the individual mobilities. The quantity K will be referred to below as simply the "mobility." It is assumed that K is constant throughout the interelectrode region and there are no ion losses as the ions traverse the distance between the electrodes, i.e., $\vec{J}$ is conserved.

The concentric wire-and-cylinder electrode geometry was considered as a candidate design for an apparatus because it had been extensively studied; a theoretical relationship between corona current and applied voltage was first given by Townsend[7]. Employing pure gases, the current-voltage data obtained with coaxial electrodes can be fitted to a theoretical expression using the mobility as a fitting parameter[8]. With the mobility so determined, the electric field at the surface of the cylinder, where an electric field probe would be positioned, could be calculated from an expression[8,9] derivable from Eqs. (1) and (5)

$$E^2 = \frac{1}{R^2}\left[r_1^{\,2}\, E^2(r_1) + \frac{I}{2\pi\varepsilon_o K}\,(R^2 - r_1^{\,2})\right] \tag{6}$$

where R is the radial distance of the cylinder from the center of the wire, r_1 is the radial distance where E begins to decrease from the breakdown value, $E(r_1)$, and I is the measured corona current per unit length of wire.

In examining the above theory and procedure, however, the following points suggest that an alternative approach be sought.

(1) No direct measurement of the electric field profile near the wire has ever been performed and, consequently, it is not clear what value r_1 should actually have. In the case of positive corona, the wire is surrounded by a glowing sheath, but there is no reliable quantitative theory describing this region. The glowing region is believed to be the source of positive ions. The outer edge of the visible sheath has sometimes been taken to be r_1, but the validity of this assumption is not known.

The situation appears to be significantly different for the case of negative corona because the sheath is now replaced by many individual glow points on the wire's surface. The wire is now an emitting surface for electrons which can subsequently attach to electronegative molecules. The negative molecules formed near the wire then drift to the outer electrode. Once again, the value to be taken for r_1 is not clear; from the above description, however, it appears that r_1 would be different for opposite polarity corona.

(2) In deriving Eq. (6), it was assumed that the mobility of the charge carrier was independent of the electric field strength. The assumption breaks down, however, if the energy gained by the ion from the field between successive collisions is comparable to the average thermal energy of the host gas[10]. This condition does, in fact, exist in the high field region near the wire. It is, therefore, not clear that the determination of the fitting parameter, K, described earlier can yield a number that can be treated as an "effective mobility".

(3) Use of a cylindrical field generating apparatus to evaluate an electric field probe will also be made difficult because a good geometrical match between the curved cylindrical surface and the typically flat electric field probe will not be possible. Measurements in our laboratory have shown that a $\sim$1 mm displacement of a vibrating-plate type probe above or below the surface of the ground plane of a parallel plate electric field apparatus (space charge free) affects the electric field reading by several percent. Thus, some error will be introduced with an apparatus having a circular geometry.

The difficulty posed by the last point can be eliminated by use of a square coaxial geometry, but the uncertainties associated with calculation of the electric field strength, i.e., items (1) and (2), remain a problem.

Another design for an apparatus which was examined and finally adopted is a parallel plate electrode system similar, in principle, to one reported by Withers et al.,[11] and employed for charging aerosols. A schematic view of our apparatus, which is much larger than the Withers system, is shown in Fig. 1. Corona wires instead of points for producing space charge and an additional ion control grid are other differences.

Ions generated by thirty 0.0057 cm diameter stainless steel corona wires are directed both upward (to the cap) and downward 8 cm to the first screen. Charge carriers not collected on the first screen continue downward another 8 cm to the second screen which is the top "plate" of a parallel plate system. The charge carriers which pass through the top plate travel a distance d to the bottom plate and form the current density $\vec{J}$.

The first screen consists of crossed 0.03 cm diameter tinned copper wire mounted on an aluminum frame 1.6 m x 1.6 m. The square openings are 1 cm x 1 cm. The second screen is an aluminum window screen with

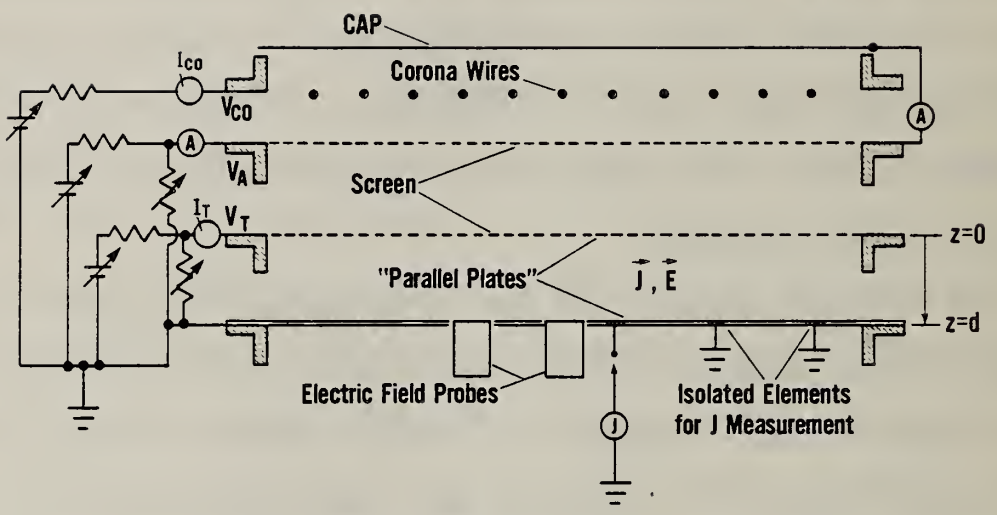

Figure 1. Schematic view of apparatus. The configuration shown is appropriate for generating an electric field with positive space charge. The top and bottom plates of the parallel plate structure are located in the planes z=0 and z=d. The corona wires are oriented parallel to one another and are perpendicular to the plane of the figure.

0.02 cm diameter wire and square openings of approximately 0.12 cm x 0.12 cm. This screen was also mounted on a 1.6 m x 1.6 m aluminum frame and stretched to provide a nearly flat surface. The bottom plate consisted of nine aluminum plates 0.2 cm thick mounted on a 1.6 m x 1.6 m aluminum frame and electrically grounded. The electrodes above the ground plane were energized using dc power supplies and biasing resistor networks as shown schematically in Fig. 1. The total corona current as well as currents to the cap and screens were monitored. Three electrically isolated current sensing elements, having areas of approximately 100 cm^2 were mounted on the bottom plate for measurements of J. The current sensing elements were within 0.01 cm of the plane defined by the bottom plate. An electrometer was used for the current measurements in the ground plane. The current density profile was measured with a moveable circular probe 6 cm in diameter with a 2 cm wide guard band. The voltages were measured with uncertainties of less than 0.5% using electrostatic voltmeters. Because the ions are produced in a region external to the parallel plates, the uncertainties associated with the choice of r_1 and the influence of excessively high electric fields on the ion mobility are avoided. The flat surface of the bottom plate also permits a good geometrical match between the ground plane and an electric field probe.

Two holes near the center of the bottom plate permitted the placement of two field probes in the ground plane for comparisons of simultaneous measurements. Each vibrating plate probe was compared with the field mill. The field mill used in this study has two signal outputs, a linear ac signal and a logarithmic dc signal which is obtained with phase sensitive circuitry. Phase sensitive detection circuits are also employed in both vibrating-plate probes.

The electric field between the parallel plates must still satisfy Eqs. (1) and (5). Solving for ρ in Eq. (5) and substituting into Eq. (1), yields for the one dimensional case,

$$\frac{dE}{dz} = \frac{J}{\varepsilon_o K E} \quad . \tag{7}$$

Solution of this differential equation gives

$$E = \sqrt{E_o^2 + \frac{2Jz}{K\varepsilon_o}} \tag{8}$$

where E_o is the electric field at the top plate, z=0. With the planes z=0 and z=d at potentials V_T and 0 respectively, Eq. (8) can be integrated, using $\vec{E}=-\nabla V$, to give a useful relation between E_o, K and J,

$$\frac{3JV_T}{K\varepsilon_o} = (E_o^2 + \frac{2Jd}{K\varepsilon_o})^{3/2} - E_o^3 \quad . \tag{9}$$

Other useful relations are found from Eqs (8) and (9) when the current density in the parallel plate region is limited by space charge. Then E_o=0 so that

$$E = \sqrt{\frac{2J_s z}{K\varepsilon_o}} \tag{10}$$

and

$$K = \frac{8}{9} \frac{J_s}{\varepsilon_o} \frac{d^3}{V_T^2} \tag{11}$$

where J_s is the space charge limited current density. When K [Eq. (11)] is substituted into Eq. (10) we have that the field at the bottom plate is

$$E(z=d) = \frac{3}{2}\left(\frac{V_T}{d}\right) \tag{12}$$

and independent of J_s value.

That the problem can be characterized as one-dimensional in Eqs. (7)-(12) can be justified if the current density profile is made sufficiently uniform in the region of interest. Then, because of the initially uniform space-charge-free field, no field component orthogonal to the z-axis will exist (except in the area of fringing fields far from the site of the measurements) and the electric potential will change throughout the region according to

$$V(z) = V_T - \frac{K\varepsilon_o}{3J}\left[\left(E_o^2 + \frac{2Jz}{K\varepsilon_o}\right)^{3/2} - E_o^3\right] . \tag{13}$$

Thus, a field probe within this region will view an electric field with a perimeter boundary condition characteristic of an infinite parallel plate system. Experimental results which indicate that this condition has been reasonably approximated are presented in the next section. It is noted that on the scale of the closely spaced holes in the top plate, it can be shown that the individual ion "beams" will overlap because of diffusion as the ions traverse the distance to the bottom plate[12].

The strategy originally adopted for generation of a calculable dc electric field with space charge involved several steps: (1) The quantity K

was to be determined in situ by measuring[11] J_s for a specific V_T and employing Eq. (11). An in situ measurement of K is required because small amounts of gases such as CO_2 and H_2O can cause significant changes in the predominant charge carrier species[5,6]. (2) Witn K determined, the quantity E_o would be obtained for arbitrary J and V_T using Eq. (9). (3) Finally, the electric field would be calculated with Eq. (8) using the values of E_o, J and V_T from step 2. How this approach had to be modified is discussed in the next section.

III. EXPERIMENTAL RESULTS AND DISCUSSION

A. Current Density Profile Measurements

Typical measurements of the current density for positive space charge as a function of position at the bottom of the parallel plates are shown in Fig. 2. The measurements were performed at 56 locations with the moveable circular probe. Forty-four values within a circular area of 0.7 m radius were averaged and the J values shown are normalized with respect to this average. An electrostatic field of 8 kV/m (i.e., $V_T \simeq 800$ volts and d = 0.10 m) existed prior to the introduction of the space charge; the average current density was near 0.2×10^{-6} A/m^2 and the total corona current, I_{co}, was near 0.6 mA. Temporal fluctuations of J were typically less than ±2%. Ignoring these fluctuations, it can be seen that within a radius of 0.7 m, the current density does not deviate from the average value by more than ±6.5%. Within a radius of 30 cm the spread in J values is less than ±3%. Current density profiles measured at other voltages and current densities with parallel plate spacings near 10 and 15 cm were similar to those shown in Fig. 2. Comparable results were obtained with negative space charge.

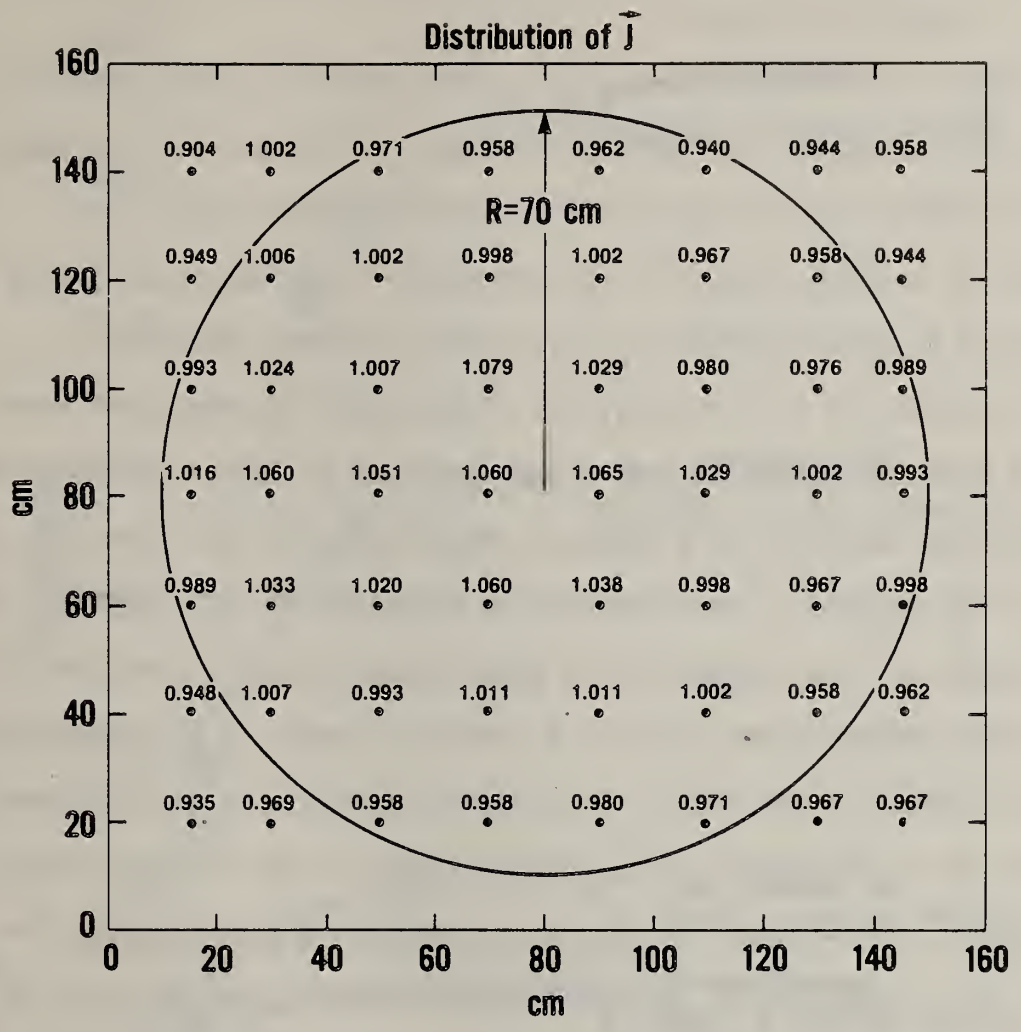

Figure 2. Measurements of the current density on the surface of the bottom plate. The results were obtained with a movable circular probe 6 cm in diameter with a 2 cm wide guard band and normalized with respect to the average of 44 measurements within a distance of 0.7 m from the center. The average J value is near 0.2×10^{-6} A/m^2.

B. Current Density and Mobility Measurements Under Space Charge Limited Conditions

Figure 3 shows measurements of J_s with positive space charge for values of V_T ranging from 400 V to 1000 V. All current density measurements were performed near the center of the bottom plate as the current incident on the top plate, I_T, was increased. This was accomplished by increasing V_A while keeping $(V_{co}-V_A)$ nearly constant (see Fig. 1).

Also shown in Fig. 3 are values of the mobility determined from Eq. (11). Evident from the values in Fig. 3 and confirmed by additional measurements at higher values of V_T is a downward trend in K as V_T is increased. At 2000 V, for example, K is calculated to be near 1.4×10^{-4} $m^2/V \cdot s$. An explanation of this downward trend would seem to exclude a mechanism involving the actual change in the value of K barring a change in air composition. That is, growth in the size of the charge carriers with an associated decrease in mobility is believed to occur in some cases as the time-of-flight is increased[13]. The trend observed here, however, is just the opposite. Much of the noted trend can be explained by more careful consideration of the potentials encountered by a charge carrier as it passes through the top plate.

It is recalled that when Eq. (11) is determined from Eq. (8), the boundary conditions invoked are that the top plate (screen) is at potential V_T and the bottom plate is at zero potential. While the potential at the bottom plate is well defined, the experimental conditions necessary to achieve a space-charge-limited current density in the parallel plate region leads to a significant perturbation of the potential experienced by the charge carrier as it passes through the screen forming the top plate. For example, when V_T is equal to 800 V, V_A must be increased to near 9 kV in order for J to become space charge limited.

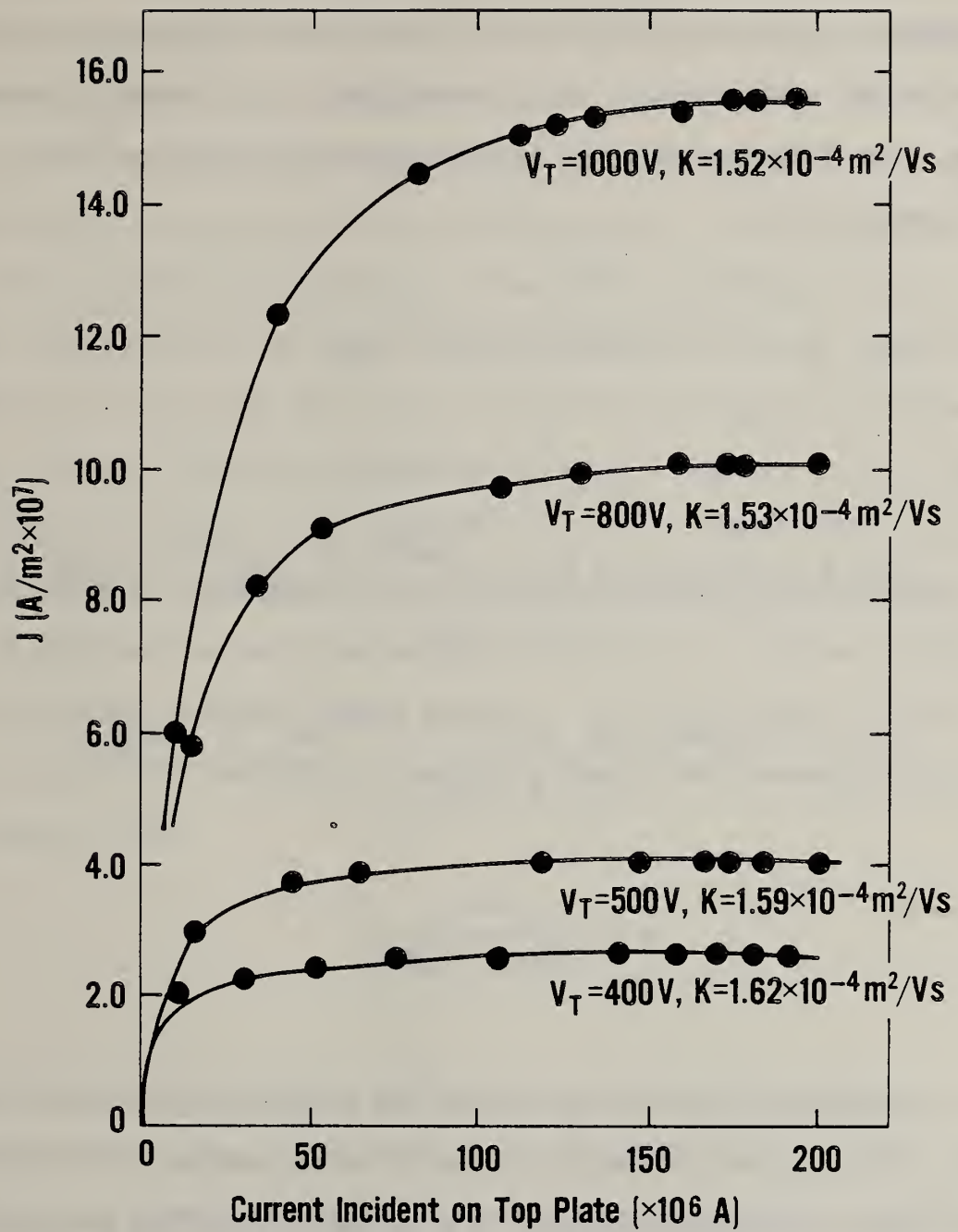

Figure 3. Measurements of space charge limited current density. The current density near the center of the bottom plate was monitored as the current incident to the top plate (screen) was increased. Also shown are values of mobility calculated from Eq. (11).

An expression which has been used to obtain an approximate[14] graphical view of conditions near the screen for this situation is one that is used for obtaining the equipotentials for a triode tube in the absence of space charge. The equipotentials are determined from the equation[15] for the potential, V(z,y)

$$V(z,y) = V_T F_1 + V_A F_2 \tag{14}$$

where

$$F_1 = \mu \frac{d_1 + z - (P/4\pi d_2)(d_2 + d_1) \ln\{e^{4\pi z/P} + 1 - 2e^{2\pi z/P} \cos(\frac{2\pi y}{P})\}}{d_1 + d_2 + \mu d_1}$$

$$F_2 = \frac{d_1 + z + (P/4\pi d_2)\, \mu d_1 \ln\{e^{4\pi z/P} + 1 - 2e^{2\pi z/P} \cos(\frac{2\pi y}{P})\}}{d_1 + d_2 + \mu d_1}$$

$$\mu = \frac{-2\pi d_2}{P \ln\{2\sin(\frac{\pi R}{P})\}} ,$$

d_1 is the parallel plate spacing, d_2 is the distance to the screen above z=0, P is the spacing of the grid wires, R is the radius of the grid wire and y is the coordinate orthogonal to z. Equation (14) has been derived assuming that the positive z direction is opposite to that shown in Fig. 1, the grid wires are parallel, infinitely long and $R \leq P/20$. The actual screen has a square mesh with spacing, P, equal to 0.14 cm and a value of R equal to 0.014 cm, i.e., R = P/10. Consequently, the amount of field penetration predicted by Eq. (14) may be somewhat excessive.

Shown in Fig. 4 are plots of equipotentials when V_A is 8 kV and the potential of the grid is 800 V. For this model calculation an ion passing through the plane of the screen experiences a space potential near 835 V which is significantly greater than the measured potential of 800 V. The 800 V equipotential plane is now 0.285 cm below the grid. If the assumption[16] is made that E=0 within ~0.1 cm below z=0 when $J=J_s$ the results in Fig. 4 suggest that a value of V_T larger than that measured with the electrostatic voltmeter should be used in Eq. (11). Calculations with Eq. (14) show, however, that the relative perturbation of V_T will diminish as V_T is increased. Use of such modified values of potential in Eq. (11) could yield a value for mobility which is independent of the voltage applied to the top plate.

The model was tested experimentally for a range of applied voltages with negative and positive charge carriers. Monitoring the dc signal, the field mill was first employed to measure E when J was space-charge-limited. Then from Eq. (12),

$$E(z=d) = \frac{3}{2}\frac{V_{sp}}{d} \qquad (15)$$

the effective space potential, designated V_{sp}, encountered by the charge carriers as they passed through the top plate was calculated. When mobilities are determined with V_{sp} instead of the potential V_T applied to the grid of the top plate, the downward trend in K is eliminated. Values of mobility calculated with Eq. (11) for applied potentials V_T and corresponding space potential V_{sp} are listed as K' and K respectively in Table I. The results represent two sets of measurements obtained on different days.

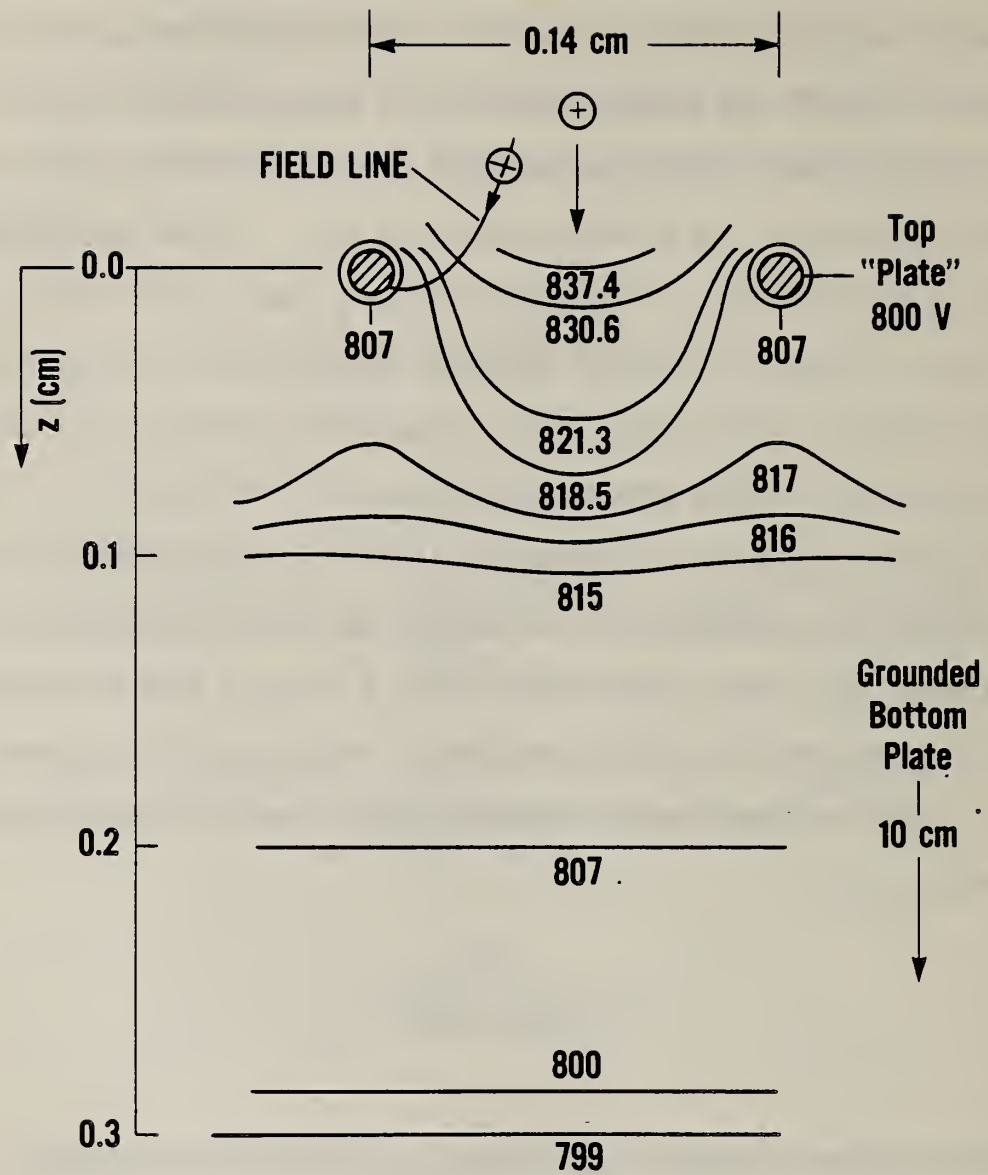

Figure 4. Two dimensional plot of equipotentials near a screen of parallel wires. The field is assumed to be Laplacian (i.e., space charge free). Nominal fields of 100 kV/m and 8 kV/m are assumed in the regions above and below the screen (top plate) respectively. The potential of the screen is taken to be 800 V.

TABLE I SPACE CHARGE MOBILITIES

d = 0.099 m T = 25.2 °C Rel. Humidity $\sim$ 50%

Negative Space Charge

$J_s(A/m^2)$	$V_T(V)$	$K'(m^2/V\ s)$	V_{sp} (V)	$K(m^2/V\ s)$
0.725×10^{-6}	- 595	2.01×10^{-4}	- 648	1.70×10^{-4}
1.90	-1003	1.85	-1036	1.73
2.66	-1209	1.79	-1238	1.71
3.86	-1497	1.69	-1491	1.71
6.33	-2013	1.54	-1939	1.66

Positive Space Charge

$J_s(A/m^2)$	$V_T(V)$	$K'(m^2/V\ s)$	V_{sp} (V)	$K(m^2/V\ s)$
0.569×10^{-6}	595	1.58×10^{-4}	658	1.29×10^{-4}
1.59	1003	1.56	1070	1.37
2.29	1209	1.54	1269	1.40
3.40	1497	1.49	1514	1.46
5.83	2013	1.41	1974	1.47

The negative mobilities, K, are independent of applied voltage from approximately -600 V to -1500 V where V_{sp} has a value slightly less than the applied potential. The calculated values of V_{sp} are less than V_T when V_T exceeds -1500 V because the measured field values show less than 50% enchancement [Eq. (15)]. In terms of the above discussion on space potentials, the condition $V_{sp}<V_T$ must be considered as physically not possible. The difficulty, however, appears not to be in the functioning of the field probe but in the operation of the apparatus. For constant mobilities, it can be shown from Eq. (11) that

$$\frac{J_s(V_1)}{J_s(V_2)} = \left(\frac{V_1}{V_2}\right)^2 \quad . \tag{16}$$

where the V's are now taken to be values of space potential. For there to be a 50% field enhancement when V_{sp} = -2013 V, for example,

$$J_s(-2013\ V) = J_s(-1238\ V)\left(\frac{2013}{1238}\right)^2 \quad .$$

Using the J_s(-1238 V) value from Table I, we have that J_s(-2013 V) should be near 7.0×10^{-6} A/m^2. The experimental value is 6.33×10^{-6} A/m^2 and as a result a smaller electric field is produced. Why the value of J saturates before acquiring the theoretically expected magnitude is not clear. Evidently the

assumption that a diffusion mechanism[16] can provide sufficient space charge between the parallel plates so that J is space charge limited is no longer valid.

Measurements of the negative space charge mobility were also made with a parallel plate spacing near 0.15 m for applied voltages between -807 V and -1086 V and were found to be in good agreement with the values in Table I. The mobility values are also in good agreement with average negative air ion mobilities reported by other investigators[17].

Because of uncertainties in the measurement of J_s, d, and E [Eq. (15)], the tabulated values of negative space charge mobility between applied voltages of -595 V and $\sim$ -1497 V are estimated to be accurate within ±7%. This estimate includes the uncertainty in the correct choice for J_s within a central circular region of radius 0.4 m on the bottom plate. The precision of the results is estimated to be near ±3%.

Table I shows that while the downward trend with applied voltage of positive space charge mobility has been eliminated, an upward trend has taken its place. The condition $V_{sp}<V_T$ also occurs with positive space charge, but at a higher applied voltage between 1500 V and 2000 V. Additional measurements have shown that $V_{sp}<V_T$ first occurs near an applied voltage of 1750 V with a corresponding current density of $\sim 4.4 \times 10^{-6}$ A/m^2.

In light of the constant negative space charge mobility measurements, the upward trend in K for positive space charge does not appear to be an artifact of the apparatus. An "aging" mechanism in which the size of the charge carrier grows as the time-of-flight between the plates increases is consistent with the data. The resulting decrease in K is compatible with the view that the predominant charge carriers produced by positive corona in laboratory air are hydrated protons,[5] i.e., $(H_2O)_n \cdot H^+$ which can grow in

size as a function of time-of-flight or distance travelled.

Measurements of positive space charge mobility were also made with a parallel plate spacing near 0.15 m for applied voltages between 907 V and 1806 volts. The upward trend in the measured mobility again occurred and the mobility values corresponding to the same ratios (V_T/d) in Table I were slightly smaller in each case. The value of K was also measured when (V_T/d) $\simeq$ 10 kV/m and d = 0.3 m and was found to be near 1.28×10^{-4} m^2/Vs.

The comparisons cannot be considered conclusive evidence for the aging model suggested above, but are supportive. Because the moisture content in the room air could not be controlled, a systematic study of the model could not be made. A 20 percent decrease in air moisture did not measurably affect the values of the mobility.

The values of positive space charge mobility in Table I compare well with average mobilities in air reported by other investigators[17]. The earlier comments regarding accuracy of the negative space charge mobility measurements apply again for the positive space charge case.

Attempts to determine mobilities with the two vibrating-plate field probes were not successful. The calculated values of V_{sp} were found to be less than V_T for most of the voltages examined. Because the response of each vibrating-plate probe to the electric field is similar, only results for one of the probes are presented.

Several simultaneous measurements of the normalized electric field, with negative space charge, made with the field mill (dc signal) and a vibrating plate probe are shown in Table II; the corresponding values of V_{sp} are also given. According to the simple qualitative model depicted in Fig. 4, field

TABLE II SPACE POTENTIAL MEASUREMENTS

d = 0.099 m T = 25.2 °C Rel. Humidity $\sim$ 50%

Negative Space Charge

		Field Mill		Vibrating-plate Probe	
$J_s(A/m^2)$	$V_T(V)$	$[E(J=J_s)/E(J=0)]_m$	$V_{sp}(V)$	$[E(J=J_s)/E(J=0)]_m$	$V_{sp}(V)$
0.725×10^{-6}	- 595	1.63	- 648	1.47	- 585
1.90	-1003	1.56	-1036	1.39	- 932
2.66	-1209	1.53	-1238	1.37	-1103
3.86	-1497	1.49	-1491	1.34	-1338

enhancements in excess of 50 percent are expected when $J=J_s$. In no case does the vibrating-plate probe indicate as much as 50% enhancement for the field strengths and current densities shown. It should be noted here, however, that the current densities reported under HVDC transmission lines are much smaller than the values presently being considered. Electric fields with less space charge are considered in the next section. The vibrating-plate probes show similar discrepancies from 50% field enhancement when electric fields with positive space charge are examined.

Simultaneously monitored with the field measurements listed in Table II was the ac signal of the field mill. For each applied voltage, the normalized field determined with the ac signal exceeded the corresponding field determined with the dc signal which is produced with phase sensitive circuitry. The difference in probe response results in higher values of V_{sp}. The higher normalized electric field and associated space potentials are considered to be an instrumental artifact. When $J\neq 0$, contributions from the space charge conduction current will add to the charge induced in the field mill sensing element by the electric field. The artifact interpretation is also supported by an examination of the higher V_{sp} values. Knowledge of V_A, V_T, and J impinging on the top plate permit an estimate of the electric field in the region above the top plate (Fig. 1). Approximate calculations of V_{sp} using Eq. (14) indicate that the space potential values determined from the ac signal are too high. Because the conduction current signal is in quadrature[3(b)] with respect to the induced signal, the phase sensitive detection circuitry eliminates the above source of error from the dc signal of the field mill.

Finally, in closing this section it is noted that the use of the field mill to determine K means that the goal of calculating the electric field from "first principles" has been abandoned. The parallel plate apparatus can still be used, however, for the evaluation of electric field probes. The use of a probe to determine physically reasonable values of K (or V_{sp}) can be regarded as one test of the instrumentation. A comparison between calculated [Eqs. (8) and (9)] and measured field values when the current density is not space charge limited represents another test. Such comparisons are described in the next section for the two types of probes.

C. Comparisons of Calculated and Measured Electric Field Strengths

Calculations of electric field strength with negative and positive space charge were performed for arbitrary values of J and V_T and compared with measurements obtained simultaneously with the field mill and vibrating plate probes. The values of K were determined using the field mill (dc signal); E_o and E were found from Eqs. (9) and (8) respectively. As noted in the previous section, the positive space charge mobility appears to change with charge carrier time-of-flight or applied voltage. The change in K as a function of applied voltage is not rapid, however, and its use for field calculations is permitted if a greater uncertainty can be tolerated in the calculation (see Sec. C.2). Only mobility values determined when $V_{sp}>V_T$ are used in the calculations for both polarity space charge. The electric potential in Eq. (9) is taken to be the applied voltage V_T in all cases because the fields above and below the top plate are comparable in magnitude when J is less than J_s.

It is noted that calculations of the electric field with space charge of either polarity are somewhat "forgiving." Uncertainties in J, d, and K tend to cancel one another during the determination of E_o [Eq. (9)]. Two

uncertainties associated with J, i.e., its relation to the average J value and the area of the sensing element, are decreased because of division by K in Eqs. (8) and (9). When the electric field is determined from Eq. (8), the square root operation further reduces the uncertainties.

The calculated normalized field values with negative space charge presented below are estimated to be accurate to within ±2%. The calculated normalized field values with positive space charge have an added uncertainty because of the upward trend in the mobility values. The accuracy of the calculation is related to the choice of K value and is discussed later. All normalized field measurements have been performed with uncertainties of less than ±1.5%.

C.1 Negative Space Charge

Comparisons between the calculated normalized field values, $[E(J\neq0)/E(J=0)]_C$, and the corresponding measured values using the field mill and a vibrating-plate probe are shown in Figs. 5 and 6. The mobility values used for field calculations in each case were determined when V_T = -1003 V. The field mill data in Fig. 6 show very good agreement with the calculations but appear to be systematically higher than the calculated values in Fig. 5. For the current densities shown there is poor agreement between the calculations and the vibrating-plate probe measurements in each case.

A possible explanation for the slightly high field mill values in Fig. 5 may be related to an effect not previously discussed, but initially observed as a "zero drift" in the instrumentation when the space charge was turned off after mobility measurements. It was later learned that the "zero drift" was actually due to the presence of a residual charge on the aluminum screen forming the top plate. The magnitude of this surface charge decayed very slowly, even when the top plate was directly connected to ground[18].

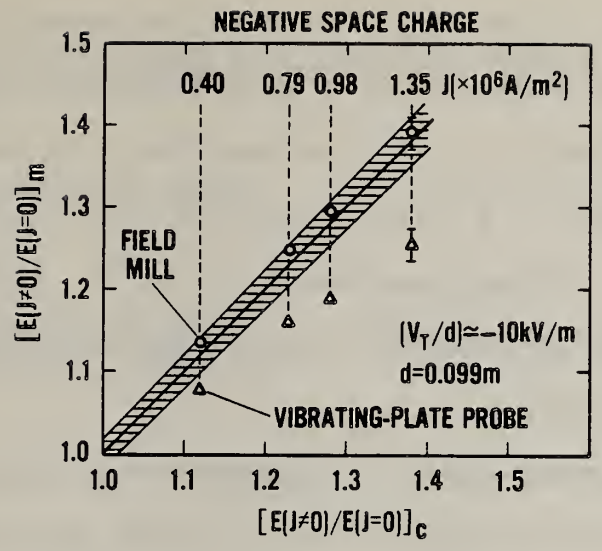

Figure 5. Comparisons between calculated and measured normalized electric field strengths when $(V_T/d) \simeq -10$ kV/m. The solid line corresponds to exact agreement and the shaded area represents the uncertainty in the calculation. Typical error bars for the measurements are also shown.

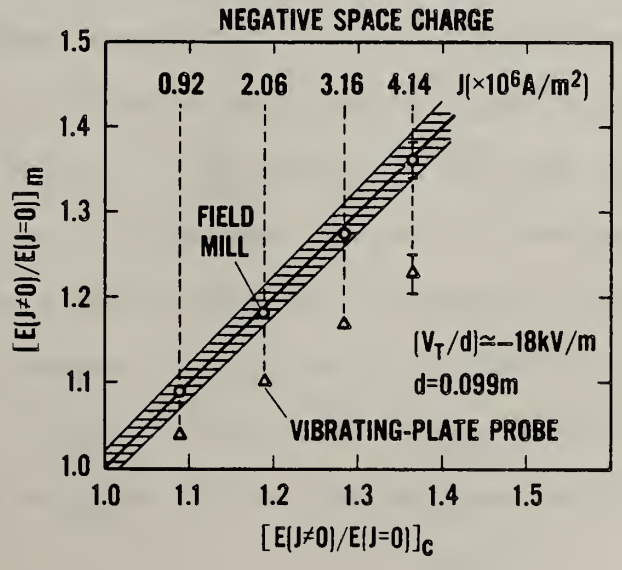

Figure 6. Comparisons between calculated and measured normalized electric field strengths when (V_T/d) is increased to -18 kV/m. The solid line corresponds to exact agreement and the shaded area represents the uncertainty in the calculation. Typical error bars for the measurements are also shown.

Surface charging of the top plate may be the source of a small perturbation of V_T not detectable with the electrostatic voltmeter which monitors the potential of the aluminum frame. An increase in the value of V_T would result in a larger value of E_o [Eq. (9)] and E [Eq. (8)], and better agreement with the measurements in Fig. 5. At higher applied voltages, the relative perturbation is apparently smaller and has less influence on the calculation.

The values of current density considered in Fig. 5 and 6 are much greater than those observed in the vicinity of HVDC transmission lines. Fields with less current density but with comparable magnitudes can be generated by increasing the plate spacing and maintaining the same ratio (V_T/d). It can be seen from Eq. (11) that the current density then scales as (1/d) if the mobility is constant and $J=J_s$. Measurements of normalized electric field with the two types of probes are given in Table III for three plate spacings with $(V_T/d) \simeq 10$ kV/m.

The results in Table III show improved agreement between the field mill and vibrating-plate probe measurements as the current density is decreased. An estimate of how small J must be before the vibrating-plate probe agrees with the field mill is obtained from a plot of J_s^{-1} versus $[E(J\neq 0)/E(J=0)]_m$ for each probe; the appropriate entries from Table III are plotted in Fig. 7. The measurements appear to agree when the space charge limited current, J_s, is approximately 0.3×10^{-6} A/m^2. This conclusion is appropriate only for the vibrating-plate probe under consideration and for $(V_T/d) \simeq 10$ kV/m. This last point is discussed further when similar data for positive space charge is considered.

C.2 Positive Space Charge

Using a single value of K determined when V_T = 1003 V, calculated normalized field strengths are compared with experimental values obtained

TABLE III FIELD MEASUREMENTS WITH DIFFERENT PARALLEL PLATE SPACING

Negative Space Charge $(V_T/d) \simeq 10$ kV/m

$J(A/m^2)$	$[E(J\neq0)/E(J=0)]_c$	Field Mill $[E(J\neq0)/E(J=0)]_m$	Vibrating-Plate Probe $[E(J\neq0)/E(J=0)]_m$
d=0.3 m			
0.188×10^{-6}	1.18	1.19	1.15
0.292	1.26	1.28	1.24
0.355	1.32	1.34	1.28
0.481	1.42	1.45	1.37
0.616*	--	1.55	1.47
d=0.15 m			
0.284×10^{-6}	1.13	1.14	1.10
0.537	1.24	1.26	1.19
0.668	1.30	1.32	1.23
0.876	1.38	1.41	1.30
1.25*	--	1.56	1.42
d=0.099 m			
0.391×10^{-6}	1.12	1.13	1.08
0.775	1.23	1.25	1.14
0.958	1.28	1.30	1.19
1.32	1.38	1.39	1.26
1.90*	--	1.55	1.39

* $J=J_s$

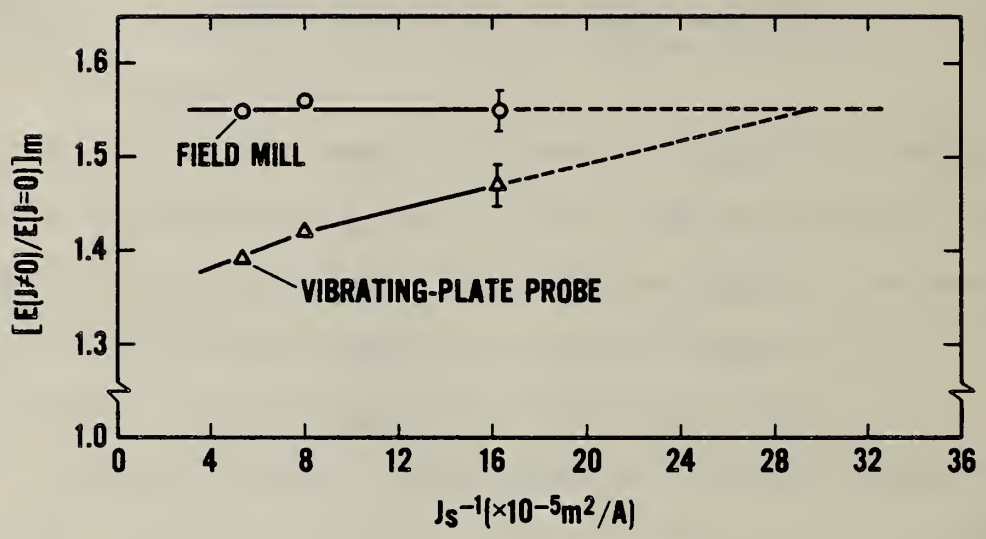

Figure 7. Intercept of two lines provides estimate of space charge limited current density for which there will be agreement between field mill and vibrating-plate probe measurements when $(V_T/d) \simeq 10$ kV/m. Typical error bars are shown.

simultaneously with the field mill and vibrating-plate probe in Fig. 8; the ratio (V_T/d) is near 10 kV/m and d=0.099 m. The poor agreement between the vibrating-plate probe measurements and the field mill results is again seen. The calculated values of the normalized field are, as in the case with negative space charge, systematically lower than the field mill data. In addition to the possible perturbation of V_T discussed previously, the use of a constant value of mobility should introduce some error in the calculations since K apparently is changing as a function of charge carrier position between the plates. This added uncertainty leads to small changes in the calculated values of E, however. If, for example, K is varied by ±2.5% from the value determined[19] at (V_T/d) = 10 kV/m, the change in E is less than ±0.6% when J is equal to 1×10^{-6} A/m^2; smaller changes occur in E for lower J values. Thus, use of a single value of K determined at the same applied voltage for the field calculations and measurements does not introduce large error.

Comparisons between calculated and measured normalized field values when V_T is increased to 1497 V are shown in Fig. 9; the mobility has been determined with an applied voltage of 1497 V. The improved agreement between the calculations and field mill measurements may again be indicative of a relatively smaller perturbation of V_T due to charging of the top plate (Section C.1).

As in the case with negative space charge, comparisons between measurements obtained with the two types of probes improved as J was decreased. Table IV shows simultaneous field measurement data for three different parallel plate spacings.

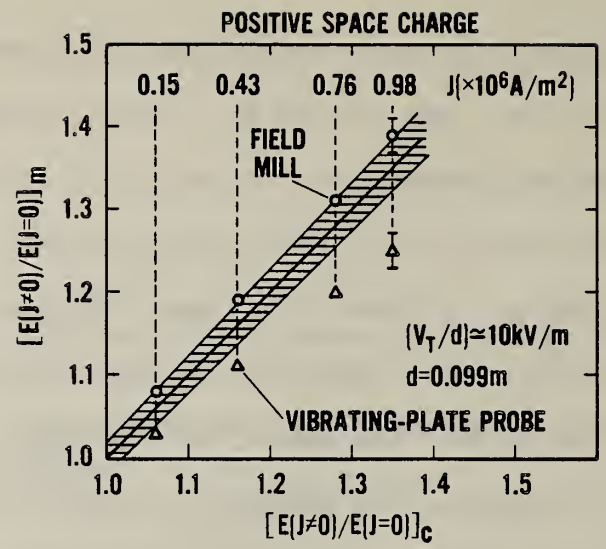

Figure 8. Comparisons between calculated and measured normalized electric field strengths when $(V_T/d) \simeq 10$ kV/m. The shaded area above the solid line has been increased to 2.6 percent to show effect on calculation if K is reduced by 2.5 percent.

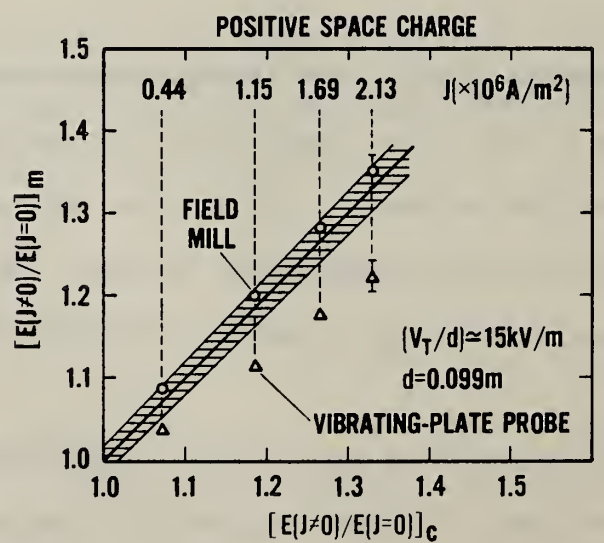

Figure 9. Comparisons between calculated and measured normalized electric field strengths when $(V_T/d) \simeq 15$ kV/m. Improved agreement between the field mill and calculated values is observed as (V_T/d) is increased.

TABLE IV FIELD MEASUREMENTS WITH DIFFERENT PARALLEL PLATE SPACING

Positive Space Charge $(V_T/d) \simeq 10$ kV/m

$J(A/m^2)$	Field Mill $[E(J\neq0)/E(J=0)]_m$	Vibrating-Plate Probe $[E(J\neq0)/E(J=0)]_m$
d=0.3 m		
0.0580×10^{-6}	1.07	1.06
0.135	1.18	1.14
0.313	1.38	1.32
0.469*	1.57	1.50
d=0.15 m		
0.080×10^{-6}	1.06	1.03
0.218	1.14	1.09
0.521	1.31	1.24
0.618	1.38	1.28
1.00*	1.59	1.45
d=0.099 m		
0.149×10^{-6}	1.08	1.03
0.432	1.19	1.11
0.758	1.31	1.20
0.984	1.39	1.25
1.58*	1.59	1.40

* $J=J_s$

Plotting the field measurements as a function of J_s^{-1}, as was done in Fig. 7 indicates that for positive space charge the vibrating-plate probe will agree with the field mill when J_s is approximately 0.26×10^{-6} A/m^2 and $(V_T/d) \simeq 10$ kV/m.

Similar measurements using the second vibrating-plate probe indicate that agreement with the field mill occurs when J_s is about 0.290×10^{-6} A/m^2. Using an older sensing head with the second field probe, measurements of the electric field revealed a greater difference from the field mill results ($J=J_s$, V_T = 1003 V, d = 0.099 m) than did the new sensing head or the first vibrating-plate probe.

A possible explanation for the low field readings observed with the vibrating-plate probes, in the presence of a space-charge current, is now briefly described[20]. Shown in Fig. 10 is a simplified schematic view of a vibrating-plate probe exposed to a dc field produced with a positive voltage, V_T. In the absence of space charge, a negative charge is induced in the vibrating plate and the operation of the probe is such that a negative feedback potential is applied to the face plate to null[3(c)] the signal V_s; the field reading is proportional to the feedback signal, V_{fb}.

If a flow of positive ions is also present, as in our measurements, V_s will acquire a positive dc component due to the voltage drop across the resistor R shown in Fig. 10. Because of the motion of the vibrating-plate, some positive voltage will be added to the feedback signal to null V_s. The smaller negative feedback voltage results in a lower field reading. Differences in the value of R due to the circuit components employed, or the surface condition of the vibrating plate could explain, in part, the differences in response of the various vibrating-plate probes.

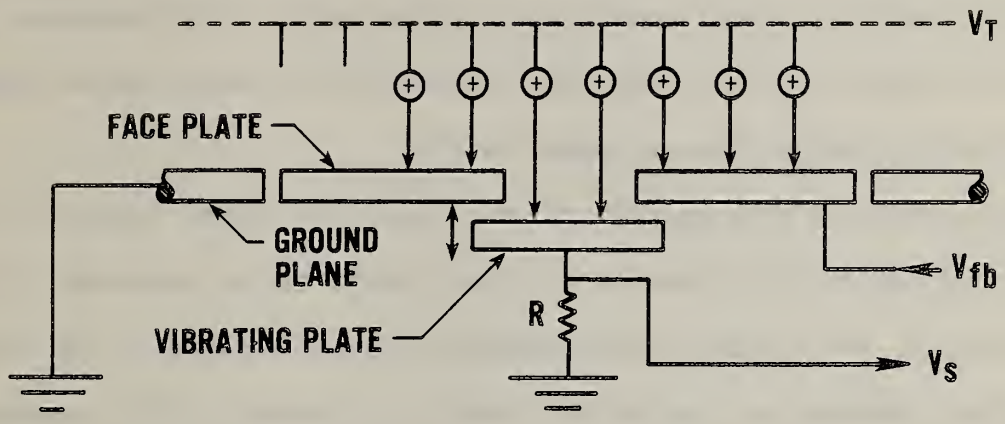

Figure 10. Simplified schematic view of vibrating-plate probe with electric field containing positive space charge. The probe responds to a field-induced negative charge on the vibrating plate by generating a negative feedback voltage and to a positive ion current incident on the vibrating plate by generating a positive feedback voltage.

IV. SUMMARY AND CONCLUSIONS

A parallel plate apparatus has been developed for generation of known dc fields with space charge and has been used to examine the performance of two types of electric field probes. Use of the probes to determine the space charge mobility provides information on the performance of the instrumentation as well as operation of the apparatus. The data indicate that a field mill with phase sensitive signal detection functions well in the presence of high current densities, but under the same conditions field probes with a vibrating-plate design give erroneous results.

With a valid in situ determination of mobility, known fields of arbitrary strength and controllable amounts of space charge can be produced. The data show that, for a given field strength, the performance of the vibrating-plate probes improves as the current density is reduced. Only examples where the space charge contribution to the total electric field strength is significant have been considered.

The laboratory measurements of electric fields described in this study must be considered as somewhat ideal because of the absence of wind, charged aerosols, and dust which are frequently encountered during outdoor measurements. The presence of wind significantly perturbs the value of J and leads to large temporal fluctuations in the field value[1]. If charging of a field probe can result in measurement errors, charged dust and aerosols will aggravate the problem[21]. In closing, we note that the results presented above appear to be the first reported comparison between calculated electric field values ($J \neq 0$) in a parallel plate apparatus -- with estimates of accuracy -- and measured field values.

V. ACKNOWLEDGEMENTS

The author is pleased to acknowledge useful conversations with J. R. Melcher, R. S. Withers, W. E. Feero and co-workers at NBS. The assistance of S. B. Kelley during the preparation of the manuscript is also greatly appreciated. This work has been supported by the Department of Energy.

VI. REFERENCES AND NOTES

1. T. D. Bracken, A. S. Capon, and D. V. Montgomery, "Ground Level Electric Fields and Ion Currents on the Celilo-Sylmar ±400 kV DC Intertie During Fair Weather," IEEE Trans. Pow. App. and Syst., Vol. PAS-97, pp. 370-378, 1978.

2. T. D. Bracken and B. C. Furumasu, "Fields and Ion Current Measurements In Regions of High Charge Density Near Direct Current Transmission Lines," in Proceedings of the Conference on Cloud Physics and Atmospheric Electricity (American Meteorological Society, Boston, 1978) p. 544.

3. For discussions of the operation of field mills see (a) W. W. Mapleson and W. S. Whitlock, "Apparatus for the accurate and continuous measurement of the earth's electric field," J. Atmosph. Terr. Phys., Vol. 7, pp. 61-72, 1955 and the references cited therein. The effect of an incident ion current on a field mill is described in (b) P. J. L. Wildman, "A device for measuring electric field in the presence of ionisation," J. Atmosph. Terr. Phys., Vol. 27, pp. 417-423, 1965. The principle of operation of the vibrating-plate field probes used during this study is found in (c) R. E. Vosteen, "D.C. Electrostatic Voltmeters and Fieldmeters," Conf. Record of 9th Ann. Meeting of IEEE Indust. Appl. Soc., October 1974.

4. O. J. Tassicker, "Boundary probe for the measurement of current density and electric field strength - with special reference to ionized gases," Proc. IEE, Vol. 121, pp. 213-220, March 1974.

5. M. M. Shahin, "Mass-Spectrometric Studies of Corona Discharge in Air at Atmospheric Pressures," J. Chem. Phys., Vol. 45, pp. 2600-2605, 1966.

6. M. M. Shahin, "Nature of Charge Carriers in Negative Coronas," Appl. Optics, Supple. No. 3 on Electrophotography, pp. 106-110, 1969.

7. J. S. Townsend, Electricity in Gases (Oxford Univ. Press, New York, 1915).

8. H. Albrecht and E. Wagner, "Measurements and Calculations In A Cylindrical Corona Discharge," 11th International Conference on Phenomena in Ionized Gases, Prague 1973, p. 192; H. Albrecht, E. Wagner, and W. H. Bloss, "Berechnung und Messung der Entladung scharakteristik einer positiven Korona," Elektrotechnische Zeitschrift, Vol. 94, pp. 599-603, 1973.

9. J. D. Cobine, Gaseous Conductors, (New York: Dover Publications, 1958), p. 258 ff. The cgs units in this reference have been replaced by SI units.

10. E. W. McDaniel and E. A. Mason, The Mobility and Diffusion of Ions in Gases, (John Wiley & Sons, New York, 1973) pp. 4-5.

11. R. S. Withers, J. R. Melcher, and J. W. Richmann, "Charging, Migration, and Electrohydrodynamic Transport of Aerosols," J. Electrostatics Vol. 5, pp. 225-239, 1978.

12. See Ref. 10, pp. 10-12 and Ref. 11.

13. M. Cabane, P. Krien, G. Madelaine, and J. Bricard, "Mobility Spectra of Ions Created in Gases Under Atmospheric Pressure," in Electrical Processes in Atmospheres, Eds. H. Dolezalek and R. Reiter (Steinkopff, Darmstadt 1977), pp. 30-39.

14. Only an approximate treatment of the problem near the screen can be made because the charge density ρ is unknown in this region.

15. J. W. Gewartowski and H. A. Watson, Principles of Electron Tubes (Van Nostrand, Princeton, NJ, 1965), p. 150 ff.

16. When $J=J_s$, the electric field theoretically vanishes in a region ($\approx$ plane) near z=0. Most of the arriving space charge follow field lines that terminate on the top plate (screen); these field lines must lie above the region where E=0. Diffusional effects are believed to be adequate to provide sufficient space charge below z=0 to maintain the saturated current, J_s [R. S. Withers, "Transport of Charged Aerosols," Sc.D. dissertation Dept. of Elect. Eng. and Comp. Sci., Massachusetts Institute of Technology, 1978 (unpublished) p. 132]. Given the values of V_A and V_T, it is difficult to conceive of field lines (Fig. 4) from above the screen penetrating to a depth greater than the grid spacing before terminating on a grid wire. This suggests that the region where E vanishes should lie within $\sim$0.1 cm below z=0.

17. V. A. Mohnen, "Formation, Nature, and Mobility of Ions of Atmospheric Importance," in Electrical Processes in Atmospheres, Eds. H. Dolezalek and R. Reiter (Steinkopff, Darmstadt 1977), pp. 1-17. Average values

of mobility for small air ions generated with corona and various radiation sources reported in this reference range from 1.23×10^{-4} m^2/Vs to 1.40×10^{-4} m^2/Vs for positive ions and 1.70×10^{-4} m^2/Vs to 2.0×10^{-4} m^2/Vs for negative ions.

18. A number of tests confirmed the existence of the surface charge on the top plate. The "zero drift" in the field mill could be eliminated by shielding the probe with a grounded plate, producing space charge of opposite polarity with the corona wires for a short time interval, or by applying a voltage ($\sim$10 - 20 V) to the top plate with opposite polarity. The presence of charge on an aluminum surface should not be unexpected (with hindsight) because the normally present aluminum oxide surface is a good insulator.

19. Values of K determined when V_T = 803 V and V_T = 1209 V differ from the value of K when V_T is 1003 V by less than 2.5 percent.

20. We thank Mr. Bruce Williams for providing this explanation and Mr. Robert Vosteen for additional useful remarks.

21. Both manufacturers of the vibrating-plate field probes recommend periodic cleaning of the sensing heads.

NBS-114A (REV. 2-8C)

U.S. DEPT. OF COMM. BIBLIOGRAPHIC DATA SHEET (See instructions)	1. PUBLICATION OR REPORT NO.	2. Performing Organ. Report No.	3. Publication Date

4. TITLE AND SUBTITLE

Generation and Measurement of DC Electric Fields with Space Charge.

5. AUTHOR(S)

Martin Misakian

6. PERFORMING ORGANIZATION (If joint or other than NBS, see instructions)

NATIONAL BUREAU OF STANDARDS
DEPARTMENT OF COMMERCE
WASHINGTON, D.C. 20234

7. Contract/Grant No.

8. Type of Report & Period Covered

9. SPONSORING ORGANIZATION NAME AND COMPLETE ADDRESS (Street, City, State, ZIP)

Department of Energy
Office of Electric Energy Systems
12th Street & Pennsylvania Ave., N.W., Mail Stop 3344
Washington, D.C. 20461

10. SUPPLEMENTARY NOTES

☐ Document describes a computer program; SF-185, FIPS Software Summary, is attached.

11. ABSTRACT (A 200-word or less factual summary of most significant information. If document includes a significant bibliography or literature survey, mention it here)

Characterization of the electrical environment in the vicinity of high voltage dc transmission lines requires measurement of a number of electrical parameters associated with the lines. These parameters include the electric field strength with significant space charge contributions. This report describes an experimental effort to generate known dc electric fields containing controlled amounts of space charge. An apparatus which has been built for this purpose is described and two types of field probes currently used for transmission line field measurements are examined with the apparatus. Limitations on the operation of one type of probe in the presence of very large current densities are identified and discussed.

12. KEY WORDS (Six to twelve entries; alphabetical order; capitalize only proper names; and separate key words by semicolons)

Calibration; dc transmission lines; electric field; electric field meters; electric field strength; electric power transmission; measurements; space charge.

13. AVAILABILITY

☒ Unlimited

☐ For Official Distribution. Do Not Release to NTIS

☐ Order From Superintendent of Documents, U.S. Government Printing Office, Washington, D.C. 20402.

☐ Order From National Technical Information Service (NTIS), Springfield, VA. 22161

14. NO. OF PRINTED PAGES

15. Price